EGTRIB Journal
JOURNAL OF
THE EGYPTIAN SOCIETY OF TRIBOLOGY
VOLUME 21, No. 2, April 2024, pp. 93 – 104 **ISSN 2090 - 5882**
(Received November 21. 2023, Accepted in final form February 18. 2024) **jest.journals.ekb.eg**

STATISTICAL ANALYSIS ON MECHANICAL PROPERTIES OF FRICTION-STIR-WELDED SUPER DUPLEX STAINLESS STEEL SAF 2507

El-Shazly M. H.[1], Sakr Kh. M.[2], Elsoeudy R. I.[3] and Ali A. S.[3]

[1]Department of Mechanical Design and Production Engineering, Faculty of Engineering, Cairo University, Giza,
[2]Engineer Officer in the Egyptian Armed Forces,
[3]Mechanical Engineering Dept., Faculty of Engineering, Suez Canal University, EGYPT.

ABSTRACT
This work employs statistical analysis, including Analysis of Variance (ANOVA) through the Design of Experiment (DOE) approach, to systematically assess the impact of key process parameters on Friction Stir Welding (FSW) outcomes. The study focuses on modeling FSW for Super Duplex Stainless Steel SAF 2507 using Abaqus, utilizing ANOVA to understand the individual and interactive effects of parameters like tilt angle, welding velocity, rotation velocity, and axial force. Abaqus simulations offer detailed insights into the thermal and mechanical aspects of welding, followed by Response Surface Methodology (RSM) for predictive modeling and parameter optimization. The research, centered on the robust Super Duplex Stainless Steel SAF 2507 and a tungsten carbide tool, contributes valuable knowledge for enhancing FSW parameters and achieving superior weld quality in practical applications.

KEYWORDS
Analysis of Variance (ANOVA), Design of Experiment (DOE), response surface methodology, super duplex stainless steel SAF 2507.

INTRODUCTION
Friction Stir Welding (FSW) is a solid-state welding process that joins materials without melting them. It was invented by The Welding Institute (TWI) in 1991, [1]. In FSW, a rotating, non-consumable tool is plunged into the joint area between two pieces of material, typically metals, which are to be joined. The heat generated by friction between the rotating tool and the work pieces softens the material without reaching the melting point. The tool then mechanically stirs or mixes the softened material, and upon cooling, a solid-state bond is formed. As illustrated in Fig. 1, FSW modeling with the Smoothed Particle Hydrodynamics (SPH) method using Abaqus [2, 3] was employed on 6 mm thick SAF 2507 super duplex stainless steel plates. The welding process incorporated V-shape joints with a 60° groove angle and a 3 mm root face design, [4, 5], Fig. 2, the tool is designed with specific features, including a 20 mm shoulder diameter, 5.5 mm pin length, 5 mm pin tip diameter,

and a 31° tapered angle. These characteristics have been carefully chosen to meet the requirements of the FSW process and optimize its performance.

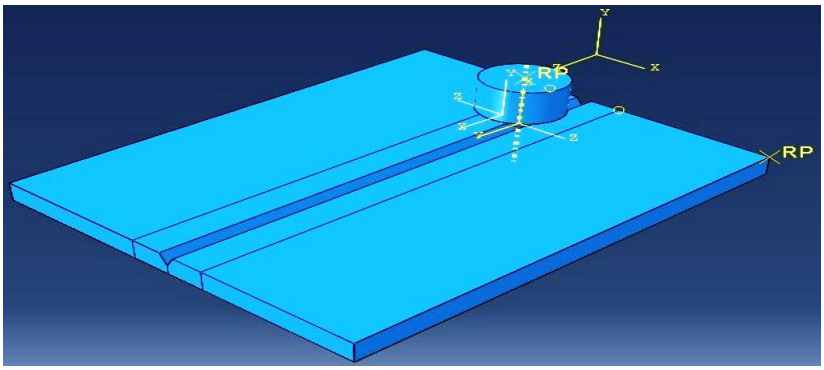

Fig. 1 Friction Stir Welding Modeling Assembly (SPH) Method.

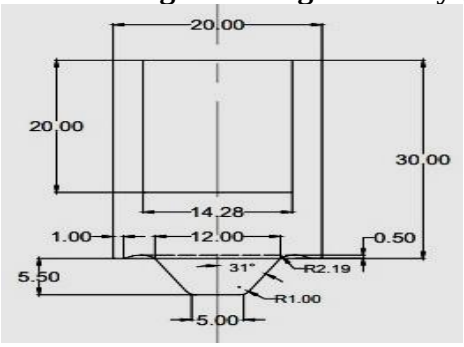

Fig. 2 Tungsten carbide tool geometry, [4].

For the Response Surface Design, we employed the central composite design (CCD) concept, [6]. CCD is an effective experimental design that helps explain multiple response variables with accuracy. This method is especially useful for constructing a second-order quadratic model without the need for an exhaustive three-level factorial experiment. By applying the CCD model to our experiment, we utilized star points to estimate curvature, allowing for a more comprehensive understanding of the relationship between the factors and the welding outcomes. This approach is widely used in response surface modeling and optimization, providing valuable insights for enhancing the friction stir welding process.

Central Composite Design for Response Surface Methodology
The formula for calculating N in the CCD model[7]is given by:

$$N=K^2 + 2K + n \quad (1)$$

Where N is the actual number of experiments, n is a number of repetition and k is the number of different factors which were incorporated within the study. Eventually, the CCD model can be best explained by the design of an expert.

Determination of α value:
The Alpha (α) value is a measure of the calculated distance of each axial point (star point) from the center in the central composite design[8]. When Alpha (α) is less than 1, it signifies

that the axial point is within the cube, and if it exceeds 1, it indicates that it lies outside the cube. In the central composite design, every factor is represented by five levels: the extremely high point (star point), higher point, center point, lower point, and the extremely low star point, [9].

To find the local axial point in the CCD model, it is essential to determine the alpha value. The choice of the alpha value influences whether the design is centered, rotatable, or orthogonal. You can calculate the alpha value using the following equation:

$$\alpha=(2k)^{0.25} \quad (2)$$

Uncoded value of alpha (α):
To determine the Uncoded value α value[10], the following equation can be used:

Uncoded value = (Coded value x L) + C (3)

Where, L = Length expressed in real units between Centre points and + 1 value of factor and C = Centre point value expressed in real units.

Process Parameters and Working Ranges
Table 1. Process parameters and their working range, [11]

Level of factor	Tilt angle	Welding velocity	Rotation velocity	Axial force
-α (Lowest)	0	12.5	250	7.5
−1 (Lower)	1	25	400	15
0(Centre point)	2	37.5	550	22.5
+1 (High)	3	50	700	30
+α (Highest)	4	62.5	850	37.5

Matrix Representation of Four -Factor Central Composite Plan
Table 2. Process Parameters and Working Ranges Overview

Standard order	Space type	Tilt angle	Welding velocity	Axial force	Velocity	Responses (Abaqus Results)		
						Max. Temp.	Von-misses stress (Pa)	Plastic strain
1	Factorial	1	25	15	400	1169	5.384E+08	2.345
2	Factorial	3	25	15	400	1262	5.422E+08	3.059
3	Factorial	1	50	15	400	1027	6.021E+08	2.281
4	Factorial	3	50	15	400	1149	6.055E+08	2.437
5	Factorial	1	25	30	400	1169	5.384E+08	2.345

6	**Factorial**	**3**	**25**	**30**	**400**	**1262**	**5.422E+08**	**3.059**
7	**Factorial**	**1**	**50**	**30**	**400**	**1027**	**6.021E+08**	**2.281**
8	**Factorial**	**3**	**50**	**30**	**400**	**1149**	**6.055E+08**	**2.437**
9	**Factorial**	**1**	**25**	**15**	**700**	**1220**	**7.712E+08**	**2.632**
10	**Factorial**	**3**	**25**	**15**	**700**	**1319**	**7.541E+08**	**2.770**
11	**Factorial**	**1**	**50**	**15**	**700**	**1023**	**7.712E+08**	**2.322**
12	**Factorial**	**3**	**50**	**15**	**700**	**1117**	**7.541E+08**	**2.190**
13	**Factorial**	**1**	**25**	**30**	**700**	**1319**	**7.712E+08**	**2.632**
14	**Factorial**	**3**	**25**	**30**	**700**	**1235**	**7.541E+08**	**2.770**
15	**Factorial**	**1**	**50**	**30**	**700**	**1023**	**7.712E+08**	**2.322**
16	**Factorial**	**3**	**50**	**30**	**700**	**1117**	**7.541E+08**	**2.190**
17	**Axial**	**0**	**37.5**	**22.5**	**550**	**977.5**	**6.039E+08**	**2.255**
18	**Axial**	**4**	**37.5**	**22.5**	**550**	**1247**	**7.038E+08**	**2.575**
19	**Axial**	**2**	**12.5**	**22.5**	**550**	**1346**	**5.878E+08**	**3.434**
20	**Axial**	**2**	**62.5**	**22.5**	**550**	**1054**	**5.245E+08**	**2.468**
21	**Axial**	**2**	**37.5**	**7.5**	**550**	**889.4**	**5.254E+08**	**2.577**
22	**Axial**	**2**	**37.5**	**37.5**	**550**	**1112**	**5.741E+08**	**2.303**
23	**Axial**	**2**	**37.5**	**22.5**	**250**	**1254**	**5.33E+08**	**2.361**
24	**Axial**	**2**	**37.5**	**22.5**	**850**	**1337**	**6.729E+08**	**2.357**
25	**Center**	**2**	**37.5**	**22.5**	**550**	**1112**	**5.741E+08**	**2.303**

Checking for adequacy of model

The reliability of the established model is evaluated through the application of the analysis of variance (ANOVA) technique, where in the results of fitting the second-order response surface model are examined. The ANOVA outcomes for temperature distribution, von-mises stresses and plastic strain are individually presented in Tables 3 to 8. To determine adequacy, the calculated F-ratio of the model is compared to the standard F-ratio from the

F-table at a 95% confidence level. If the calculated F-ratio is less than the tabulated value, the model is considered adequate within the specified confidence level.

The values of prob > F for the three developed models are all below 0.05 (95% confidence level), signifying the significance of the model and the lack of significant fit issues [12 - 15].

Response 1: Temperature
Analysis of variance
Table 3. ANOVA for Quadratic model

Source	Sum of Squares	df	Mean Square	F-value	p-value	
Model	3.500E+05	14	24997.89	14.75	< 0.0001	significant
A-Tilt angle	71613.38	1	71613.38	42.27	< 0.0001	
B-Welding velocity	1.562E+05	1	1.562E+05	92.17	< 0.0001	
C-Axial force	8258.46	1	8258.46	4.87	0.0475	
D-Rotation speed	5221.50	1	5221.50	3.08	0.1046	
AB	529.00	1	529.00	0.3122	0.5866	
AC	0.0000	1	0.0000	0.0000	1.0000	
AD	484.00	1	484.00	0.2856	0.6028	
BC	0.0000	1	0.0000	0.0000	1.0000	
BD	6889.00	1	6889.00	4.07	0.0667	
CD	0.0000	1	0.0000	0.0000	1.0000	
A^2	81.99	1	81.99	0.0484	0.8296	
B^2	12183.69	1	12183.69	7.19	0.0200	
C^2	14340.56	1	14340.56	8.46	0.0131	
D^2	48688.03	1	48688.03	28.73	0.0002	
Residual	20332.60	12	1694.38			
Lack of Fit	20332.60	10	2033.26			
Pure Error	0.0000	2	0.0000			
Cor Total	3.703E+05	26				

The Model F-value of 14.75 implies the model is significant. There is only a 0.01 % chance that an F-value this large could occur due to noise.

Fit Statistics
Table 4. Fit Statistics for Temperature Distribution

Std. Dev.	41.16	R^2	0.9451
Mean	1154.40	Adjusted R^2	0.8810
C.V. %	3.57	Predicted R^2	0.6837
		Adeq Precision	12.9635

The Predicted R^2 of 0.6837 is in reasonable agreement with the Adjusted R^2 of 0.8810; i.e. the difference is less than 0.2. Adeq Precision measures the signal to noise ratio. A ratio greater than 4 is desirable.
The ratio of 12.964 indicates an adequate signal. This model can be used to navigate the design space.
Response 2: Von-Misses Stress
Analysis of variance
Table 5 ANOVA for Linear model

Source	Sum of Squares	df	Mean Square	F-value	p-value	
Model	1.376E+17	4	3.441E+16	8.24	0.0003	significant
A-Tilt angle	8.857E+14	1	8.857E+14	0.2120	0.6497	
B-Welding velocity	6.763E+14	1	6.763E+14	0.1619	0.6913	
C-Axial force	3.953E+14	1	3.953E+14	0.0946	0.7613	
D-Rotation speed	1.357E+17	1	1.357E+17	32.48	< 0.0001	
Residual	9.190E+16	22	4.177E+15			
Lack of Fit	9.190E+16	20	4.595E+15			
Pure Error	0.0000	2	0.0000			
Cor Total	2.295E+17	26				

The Model F-value of 8.24 implies the model is significant. There is only a 0.03 % chance that an F-value this large could occur due to noise.

Fit Statistics
Table 6. Fit Statistics for Von-mises Stress

Std. Dev.	6.463E+07	R^2	0.5997
Mean	6.343E+08	Adjusted R^2	0.5269
C.V. %	10.19	Predicted R^2	0.3922
		Adeq Precision	10.8140

The Predicted R^2 of 0.3922 is in reasonable agreement with the Adjusted R^2 of 0.5269; i.e. the difference is less than 0.2. Adeq Precision measures the signal to noise ratio, a ratio greater than 4 is desirable. The ratio of 10.814 indicates an adequate signal. This model can be used to navigate the design space.

Response 3: Plastic Strain (PE)
Analysis of variance
Table 7. ANOVA for Quadratic model

Source	Sum of Squares	df	Mean Square	F-value	p-value	
Model	2.28	14	0.1629	27.34	< 0.0001	significant

A-Tilt angle	**0.2384**	**1**	**0.2384**	**40.01**	**< 0.0001**	
B-Welding velocity	**1.08**	**1**	**1.08**	**180.75**	**< 0.0001**	
C-Axial force	**0.0125**	**1**	**0.0125**	**2.10**	**0.1729**	
D-Rotation speed	**0.0075**	**1**	**0.0075**	**1.26**	**0.2841**	
AB	**0.1714**	**1**	**0.1714**	**28.77**	**0.0002**	
AC	**0.0000**	**1**	**0.0000**	**0.0000**	**1.0000**	
AD	**0.1866**	**1**	**0.1866**	**31.32**	**0.0001**	
BC	**0.0000**	**1**	**0.0000**	**0.0000**	**1.0000**	
BD	**0.0104**	**1**	**0.0104**	**1.75**	**0.2110**	
CD	**0.0000**	**1**	**0.0000**	**0.0000**	**1.0000**	
A^2	**0.0102**	**1**	**0.0102**	**1.71**	**0.2151**	
B^2	**0.5183**	**1**	**0.5183**	**86.99**	**< 0.0001**	
C^2	**0.0169**	**1**	**0.0169**	**2.83**	**0.1182**	
D^2	**0.0013**	**1**	**0.0013**	**0.2220**	**0.6459**	
Residual	**0.0715**	**12**	**0.0060**			
Lack of Fit	**0.0715**	**10**	**0.0072**			
Pure Error	**0.0000**	**2**	**0.0000**			
Cor Total	**2.35**	**26**				

The Model F-value of 27.34 implies the model is significant. There is only a 0.01 % chance that an F-value this large could occur due to noise.

Fit Statistics

Table 8. Fit Statistics for Plastic Strain

Std. Dev.	**0.0772**	**R^2**	**0.9696**
Mean	**2.49**	**Adjusted R^2**	**0.9341**
C.V. %	**3.10**	**Predicted R^2**	**0.8249**
		Adeq Precision	**21.2583**

The Predicted R^2 of 0.8249 is in reasonable agreement with the Adjusted R^2 of 0.9341; i.e. the difference is less than 0.2. Adeq Precision measures the signal to noise ratio, a ratio greater than 4 is desirable. The ratio of 21.258 indicates an adequate signal. This model can be used to navigate the design space.

Final Equations

Response 1: Temperature

Final Equation in Terms of Coded Factors

Temperature =1,112 +(54.625 * A) + (-80.6667 * B) + (18.55 * C) + (14.75 * D) + (5.75 * AB) (-2.2172e-13 * AC) + (- 5.5 * AD) +(-2.31617e-13 * BC) +(-20.75 * BD) +

(-2.21741e-13 * CD) + (1.96042 * A^2) + (23.8979 * B^2) +(-25.9271 * C^2) + (47.7729 * D^2). (4)

The equation in terms of coded factors can be used to make predictions about the response for given levels of each factor. By default, the high levels of the factors are coded as +1 and the low levels are coded as -1. The coded equation is useful for identifying the relative impact of the factors by comparing the factor coefficients.

1.1.1 Final Equation in Terms of Actual Factors

Temperature = 1,532.79 + (49.7 * A) + (-12.7577 * B) + (23.215 * C) +(-1.7489 * D) + (0.46 * AB) + (-4.32576e-14 * AC) +(-0.0366667 * AD) +(-2.86656e-15 * BC) + (-0.0110667 * BD) + (-2.06982e-16 * CD) + (1.96042 * A^2) +(0.152947 * B^2) + (-0.460926 * C^2) + (0.00212324 * D^2). (5)

The equation in terms of actual factors can be used to make predictions about the response for given levels of each factor. Here, the levels should be specified in the original units for each factor. This equation should not be used to determine the relative impact of each factor because the coefficients are scaled to accommodate the units of each factor and the intercept is not at the center of the design space.

Response 2: Von-Misses
Final Equation in Terms of Coded Factors
Von-misses = 6.3427e+08 + 6.075e+06 * A + 5.30833e+06 * B +4.05833e+06 * C + 7.51917e+07 * D (6)

Final Equation in Terms of Actual Factors
Von-Misses = 3.18318e+08 + 6.075e+06 * A + 424,667 * B + 541,111 * C + 501,278 * D (7)

Response 3: Plastic Strain
Final Equation in Terms of Coded Factors

Plastic Strain = 2.303 + (0.0996667 * A) + (-0.211833 * B) +(-0.0228333 * C) + (-0.0176667 * D) + (-0.1035 * AB) + (- 3.50823e-16 * AC) +(-0.108 * AD) +(-3.79863e-16 * BC) + (-0.0255 * BD) +(-3.92619e-16 * CD) +(0.021875 * A^2) +(0.155875 * B^2) +(0.028125 * C^2) + (0.007875 * D^2) (8)

Final Equation in Terms of Actual Factors
Plastic Strain= 3.02832 + (0.718667 * A) +(-0.0677267 * B) +(-0.0255444 * C) + (0.00144722 * D) + (- 0.00828 * AB) +(-1.2486e-16 * AC) + (-0.00072 * AD) +(-1.10085e-17 * BC) + (-1.36e-05 * BD) +(-9.934e-19 * CD) +(0.021875 * A^2) + (0.9976 2) + (0.0005 * C^2) + (3.5e-07 * D^2 (9)

Effect of process parameters on Temperature:
The plot for the response temperature of the joint is illustrated in Fig. 3. This plot provides the response surface and shows the change in temperature while each FSW parameter

moves from the reference value. Fig. 3 (a - d) illustrates the contour and 3D-surface plots presenting the interaction effect of any two input parameters on the temperature.

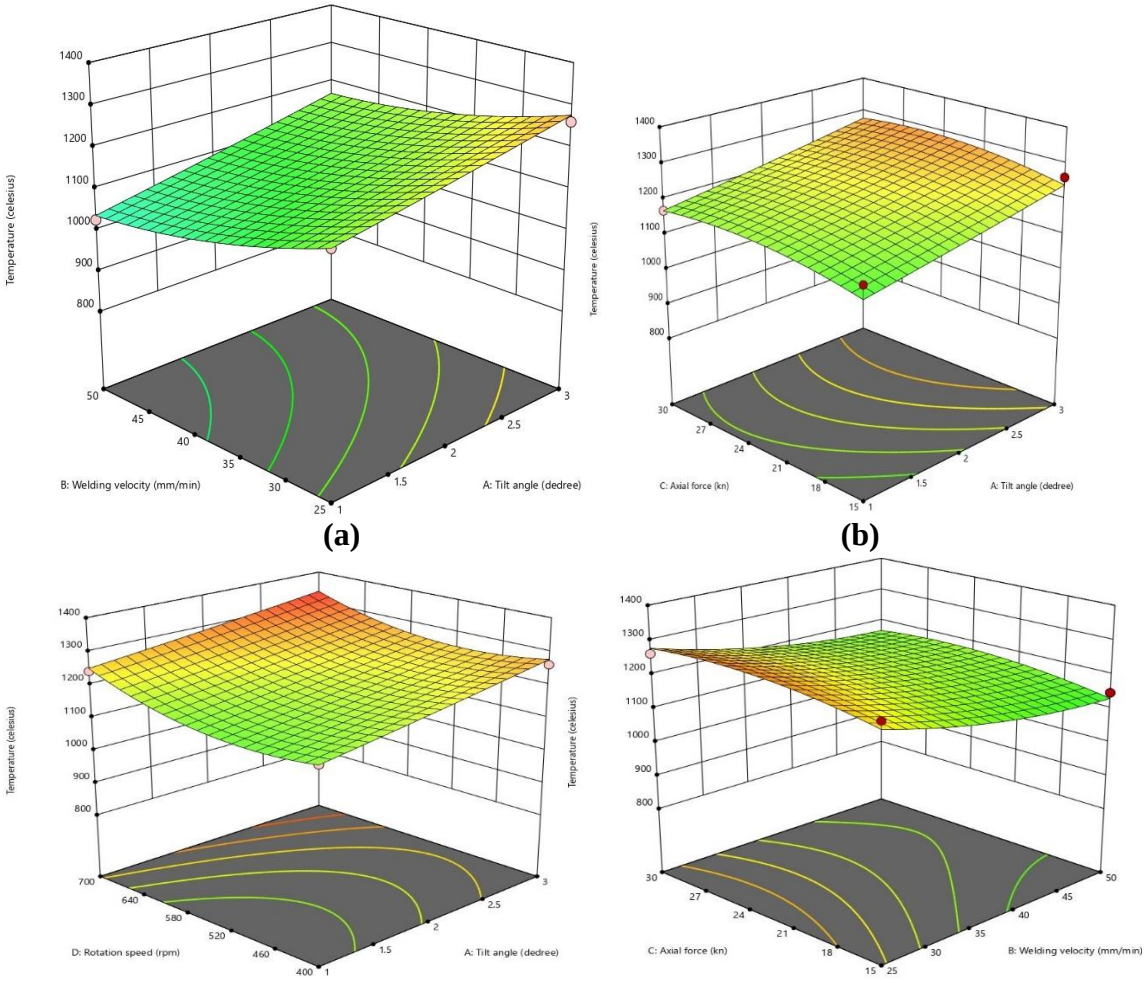

(a) **(b)**

(C) **(D)**

Fig. 3, (a - d). Contour and 3D-surface plots representing the effect of FSW parameters on temperature distribution.

Effect of process parameters on plastic strain:

The plot for the response plastic strain of the joint is illustrated in Fig. 4. This plot provides the response surface and shows the change in plastic strain while each FSW parameter moves from the reference value. Fig. 4, (a - c) illustrates the contour and 3D-surface plots presenting the interaction effect of any two input parameters on the plastic strain.

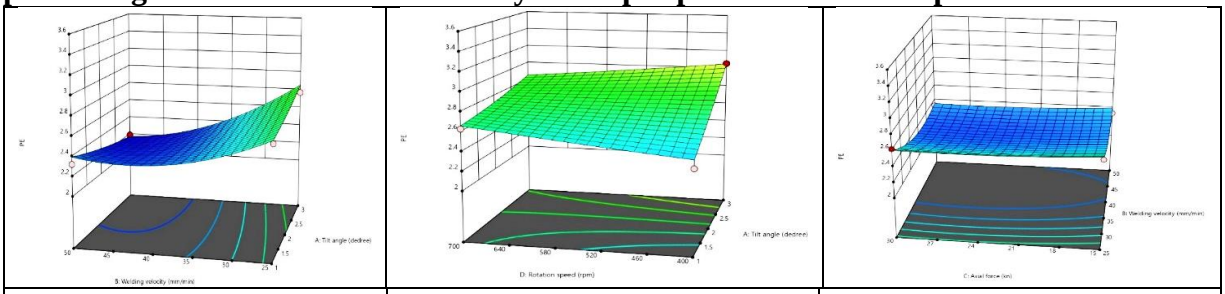

(a)	(b)	(c)

Fig. 4, (a - c) Contour and 3D-surface plots representing the effect of FSW parameters on the plastic strain.

Diagnostics

In Fig. 5, a, it is observed that the errors conform to a normal distribution, as evidenced by the straight line in the normal probability plot of residuals. Fig. 5, b illustrates the alignment of actual data and predicted values from the mathematical model along a straight line, confirming the efficacy of the regression model. The predicted model also satisfies the assumption of constant variance, as depicted by the random scatter plot in Fig. 5, c, portraying the distribution of residuals without a specific structure. Additionally, Fig. 5, d displays the random scatter of residuals around the mean value, suggesting the independence of residuals from the run order.

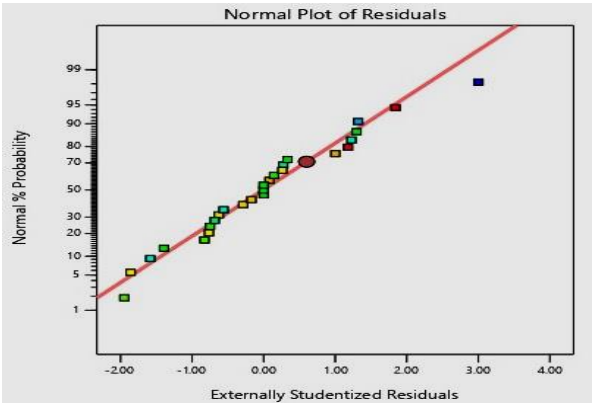

(a)

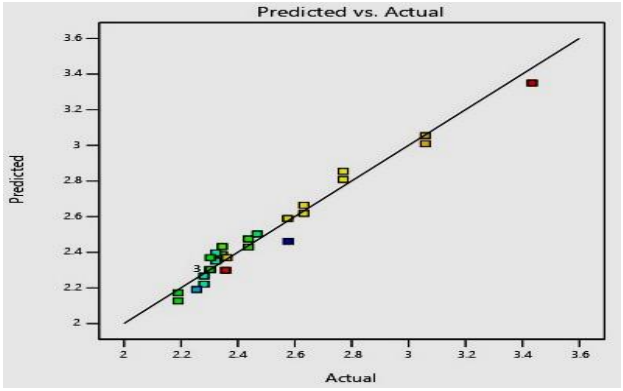

(b)

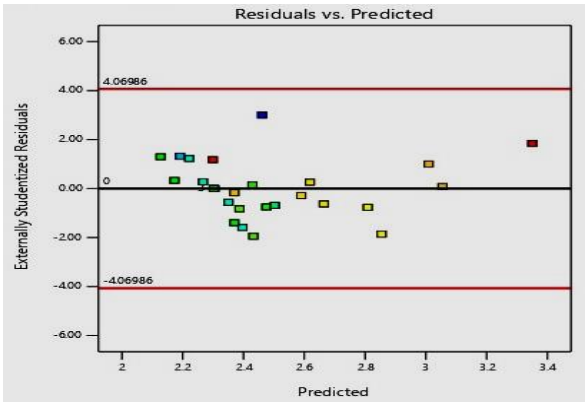

(c)

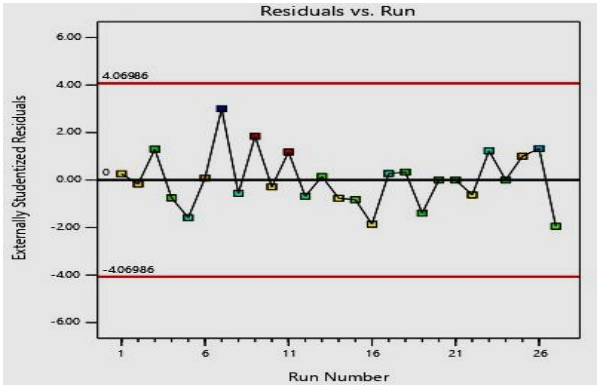

(d)

Fig. 5 Design expert response, (a) normal probability plot residuals of surface roughness, (b) the plot of actual vs. predicted response of surface roughness data, (c) the plot of residuals vs. predicted response of surface roughness data, (d) the plot of residuals vs. run of plastic strain data.

CONCLUSIONS

1. **RSM is a powerful tool in determination of factor effects.**
2. **According to the ANOVA results for temperature distribution, P-values less than 0.0500 indicate model terms are significant. In this case A, B, C, B^2, C^2, D^2 are significant model terms.**
3. **According to the ANOVA results for von-mises stress, P-values less than 0.0500 indicate model terms are significant. In this case D is a significant model term.**
4. **According to the ANOVA results for Plastic strain, P-values less than 0.0500 indicate model terms are significant. In this case A, B, AB, AD, B^2 are significant model terms.**
5. **Increase the tool rotational speed or decrease the welding speed causes increasing in the temperature. This change in temperature significantly influences the mechanical properties of the weld.**

REFERENCES

1. K. Devendranath Ramkumar et al., "Effect of optimal weld parameters in the microstructure and mechanical properties of autogeneous gas tungsten arc weldments of super-duplex stainless steel UNS S32750," Mater. Des., Vol. 66, no. PA, pp. 356–365, 2015, doi: 10.1016/j.matdes.2014.10.084, (2015).

2. B. Meyghani, M. B. Awang, and C. S. Wu, "Thermal analysis of friction stir processing

(FSP) using arbitrary lagrangian-eulerian (ALE) and smoothed particle hydrodynamics (SPH) meshing techniques," Materwiss. Werksttech., Vol. 51, no. 5, pp. 550–557, (2020).
3. K. A. Fraser, "Robust and efficient meshfree solid thermo-mechanics simulation of friction stir welding." Université du Québec à Chicoutimi, (2017).
4. Eslam A., "Friction stir welding of super duplex stainless steel", A M. Sc. Thesis, Faculty of Engineering, Suez Canal University, EGYPT, (2023).
5. M. M. Z. Ahmed et al., "Friction stir welding of 2205 duplex stainless steel: Feasibility of butt joint groove filling in comparison to gas tungsten arc welding," Materials (Basel)., Vol. 14, no. 16, p. 4597, (2021).
6. S. Bhattacharya, "Central Composite Design for Response Surface Methodology and Its Application in Pharmacy," P. Kayaroganam, Ed., Rijeka: IntechOpen, 2021, p. Ch. 5. doi: 10.5772/intechopen.95835, (2021).
7. S. Bhattacharya, "Central Composite Design for Response Surface Methodology and Its Application in Pharmacy," Response Surf. Methodol. Eng. Sci., no. January, 2021, doi: 10.5772/intechopen.95835, (2021)
8. A. Asghar, A. A. Abdul Raman, and W. M. A. W. Daud, "A comparison of central composite design and Taguchi method for optimizing Fenton process," Sci. World J., Vol. 2014, (2014).
9. A. Bevilacqua, M. R. Corbo, and M. Sinigaglia, "Design of experiments: a powerful tool in food microbiology," Curr. Res. Technol. Educ. Top. Appl. Microbiol. Microb. Biotechnol., pp. 1419–1429, (2010).
10. D. I. Ellis, D. Broadhurst, S. J. Clarke, and R. Goodacre, "Rapid identification of closely related muscle foods by vibrational spectroscopy and machine learning," Analyst, Vol. 130, no. 12, pp. 1648–1654, (2005).
11. R. G. Cooper, S. J. Edgett, and E. J. Kleinschmidt, "Optimizing the stage-gate process: what best-practice companies do—I," Res. Manag., Vol. 45, no. 5, pp. 21–27, (2002).
12. S. R. Ramasamy, J. Gould, and D. Workman, "Design-of-experiments study to examine the effect of polarity on stud welding," Weld. JOURNAL-NEW YORK-, Vol. 81, no. 2, pp. 19-S, (2002).
13. D. C. Montgomery, Design and analysis of experiments. John wiley & sons, 2017.
14. R. Kadaganchi, M. R. Gankidi, and H. Gokhale, "Optimization of process parameters of aluminum alloy AA 2014-T6 friction stir welds by response surface methodology," Def. Technol., Vol. 11, no. 3, pp. 209–219, (2015).
15. K. Elangovan, V. Balasubramanian, and S. Babu, "Predicting tensile strength of friction stir welded AA6061 aluminium alloy joints by a mathematical model," Mater. Des., Vol. 30, No. 1, pp. 188–193, (2009).